# Optical Parametric Scattering in Ammonium Dihydrogen Phosphate*

DOUGLAS MAGDE AND HERBERT MAHR
*Laboratory of Atomic and Solid State Physics, Cornell University, Ithaca, New York*

(Received 16 February 1968)

This paper presents a detailed experimental study of spontaneous parametric scattering in the optical region in ammonium dihydrogen phosphate (ADP) pumped with a pulsed laser source at 3472 Å. The dependence of the process on crystal orientation, observation direction, pump power, crystal length, and detector aperture, and the properties of bandwidth and intensity of the scattered radiation, were measured and compared with predictions of a detailed theory by Giallorenzi and Tang. The parametric process covers a wide range of visible and infrared wavelengths and can be observed over a rather large range of observation directions. For a peak power of 1 MW of the pump, about 1–10 $\mu$W of scattered radiation was obtained in a 1-cm-long crystal with a detector aperture of about $10^{-4}$ sr.

## INTRODUCTION

THIS paper presents experimental results on spontaneous parametric scattering in the optical region in ammonium dihydrogen phosphate (ADP) pumped at 3472 Å with $Q$-switched laser pulses of about 1-MW peak power. As shown schematically in Fig. 1(a), parametric scattering consists of the breakup of a pump photon $\hbar\omega_p$ into a signal photon $\hbar\omega_s$ and an idler photon $\hbar\omega_i$. Conservation of energy and momentum as required in this breakup will not, in general, be simultaneously satisfied in optical media. These two conditions, however, can be met in birefringent uniaxial crystals by making one of the waves, the pump usually, an extraordinary ray and adjusting its index of refraction and, therefore, its electromagnetic momentum. One way of doing this is by properly choosing the angle $\theta_p$ between the optic axis and the pump-beam direction [see Fig. 1(b)]. By rotating the crystal, that is, by changing the angle $\theta_p$, different pairs of signal and idler photons will be obtained. This is true for a given observation direction $\alpha$. As can be seen from Figs. 1(a) and 1(b), different signal-idler pairs can also be "phase matched" by changing $\alpha$, the angle of observation.

Parametric scattering in the optical region is only possible in *nonlinear* optical crystals, that is, in crystals which show a nonlinear dependence of the (optical) dielectric constant on the electric field strength. The scattering can be spontaneous or stimulated.

The stimulated process was first observed by Giordmaine and Miller[1] in lithium niobate pumped by 5300-Å laser pulses. They successfully operated a parametric oscillator formed by placing the active medium inside an optical cavity which enhanced the scattered intensity by successive reflections until it became strong enough to stimulate further parametric breakups. Several of these "tunable laser" sources have since been reported.[2]

The spontaneous parametric process which is investigated in this paper is of interest for two reasons: (1) The amount of spontaneous parametric scattering determines the construction details of parametric oscillators and, as "quantum noise," limits the usefulness of parametric amplifiers. (2) The spontaneous process contains all the basic physics of this particular nonlinear interaction between light waves and matter and is particularly suited for a direct comparison of theory and experiment. Most appropriate for a comparison with the experimental results of this paper is a quantum-mechanical scattering theory by Giallorenzi and Tang[3] which makes very detailed predictions of the spontaneous parametric process in the optical region. A similar theory was reported by Klyshko[4] in a brief paper.

Some of the results described in this paper were reported previously.[5] Parametric scattering with pulsed laser-pump sources was also studied by Akhmanov *et al.*[6] with potassium dihydrogen phosphate (KDP) pumped at 3630 Å. The observation of parametric scattering in $LiNbO_3$ pumped with a continuous argon

* Work supported in part by the Advanced Research Projects Agency through the Materials Science Center of Cornell University, Report No. 874 and by the U.S. Office of Naval Research, Contract No. NONR-401(47), Technical Report No. 22.

[1] J. A. Giordmaine and R. C. Miller, Phys. Rev. Letters **14**, 973 (1965); *Physics of Quantum Electronics*, edited by P. L. Kelly, B. Lax, and P. E. Tannewald (McGraw-Hill Book Co., New York, 1966), pp. 31–42.

[2] S. A. Akhmanov, A. I. Kovrigin, V. A. Kolosov, A. S. Piskarskas, V. V. Fadeev, and R. V. Khokhlov, Zh. Eksperim. i Teor. Fiz. Pis'ma v Redaktsiyu **3**, 372 (1966) [English transl.: Soviet Phys.—JETP Letters **3**, 241 (1966)]; J. A. Giordmaine and R. C. Miller, Appl. Phys. Letters **9**, 298 (1966); R. C. Miller and W. A. Nordland, *ibid.* **10**, 53 (1967); R. V. Khokhlov *et al.*, in *Modern Optics*, edited by J. Fox (Brooklyn Polytechnic Institute Press, New York, 1967), Vol. 17.

[3] T. G. Giallorenzi and C. L. Tang, Phys. Rev. **166**, 225 (1968). This article may be consulted for extensive references to previous theoretical work.

[4] D. N. Klyshko, Zh. Eksperim. i Teor. Fiz. Pis'ma v Redaktsiyu **6**, 490 (1967) [English transl.: Soviet Phys.—JETP Letters **6**, 23 (1967)].

[5] D. Magde and H. Mahr, Bull. Am. Phys. Soc. **12**, 273 (1967); Phys. Rev. Letters **18**, 905 (1967); D. Magde, R. Scarlet, and H. Mahr, Appl. Phys. Letters **11**, 381 (1967).

[6] S. A. Akhmanov, V. V. Fadeev, R. V. Khokhlov, and O. N. Chunaev, Zh. Eksperim. i Teor. Fiz. Pis'ma v Redaktsiyu **6**, 575 (1967) [English transl.: Soviet Phys.—JETP Letters **6**, 85 (1967)].

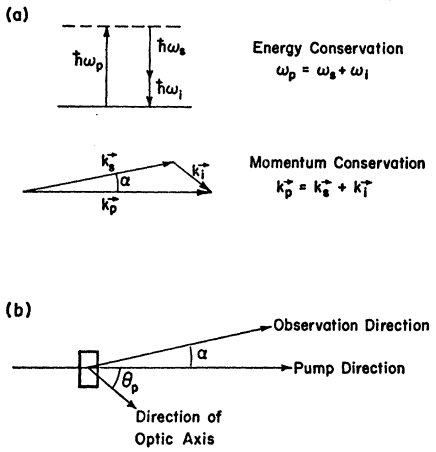


FIG. 1. (a) Parametric breakup of a pump photon $\hbar\omega_p$ into a signal photon $\hbar\omega_s$ and an idler photon $\hbar\omega_i$ under conservation of energy and momentum. (b) The forward pump-beam direction defines an angle $\alpha$ at which scattered signal or idler light is observed. It also defines the angle $\theta_p$ between the optic axis of the crystal and the incident pump radiation. It is this angle $\theta_p$ which permits one to adjust $n_p^e$, the extraordinary index of refraction of the pump light, to a desired "phase matching" value.

ion-laser source was reported by Harris *et al.*[7] and more recently by Klyshko and Krindach.[8]

## EXPERIMENTAL SETUP

The arrangement of the principal elements of the experimental setup is schematically illustrated in Fig. 2. A $Q$-switched ruby laser (TRG, Inc., Model 104) employing a rotating prism and a Daly-Sims accessory provided reproducible single pulses of approximately 30-MW peak power and 30–35-nsec duration (full width at half-power) at 6943 Å. A KDP second-harmonic generator converted the red laser pulse into a maximum of 1 MW at 3472 Å in a pulse of 20–25-nsec duration and a beam of approximately $\frac{1}{4}$ cm$^2$ area. The

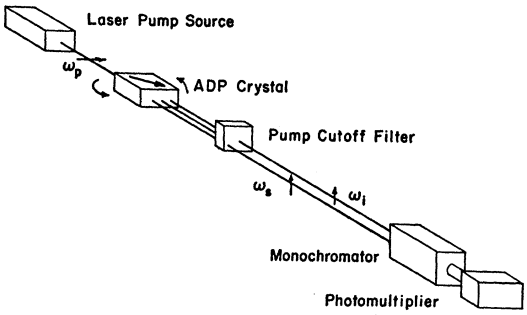


FIG. 2. Schematic of the experimental setup. The detection system could be rotated with the crystal as a pivot around the forward pump-beam direction by measured amounts $\alpha$.

[7] S. E. Harris, M. K. Oshman, and R. L. Byer, Phys. Rev. Letters **18**, 732 (1967); R. L. Byer and S. E. Harris, Phys. Rev. **168**, 1064 (1968).

[8] D. N. Klyshko and D. P. Krindach, in Proceedings of the Third USSR Symposium on Nonlinear Optics, Yerevan, 1967 (unpublished).

pump frequency bandwidth in any one shot was measured to be less than 0.08 cm$^{-1}$. Cutoff filters removed the ruby fundamental light before the ultraviolet pump-beam entered an ADP crystal at near normal incidence.

The ADP crystals investigated were obtained from Clevite Corporation, cut to size with a string saw, ground flat with aluminum oxide in ethylene glycol on glass, and polished with chromium oxide in ethylene glycol on a beeswax lap. The experimental results were not sensitive to precise surface conditions once visual transparency was obtained. The crystals were mounted on a student spectroscope table to provide rotational motion of about one minute precision.

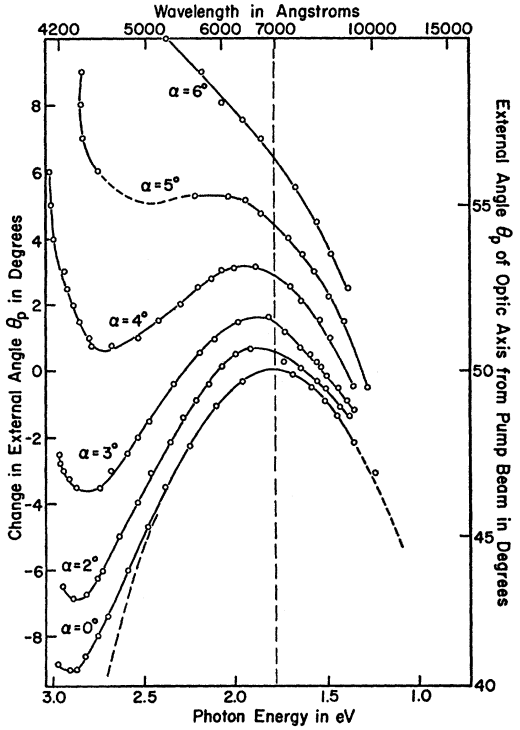


FIG. 3. Tuning curve of parametric scattering in ADP pumped at 3472 Å. The relative change in the angle $\theta_p$, measured externally in degrees, is plotted versus the photon energy of the scattered signal and idler radiation for a variety of observation directions $\alpha$. The right-hand ordinate gives the approximate angle $\theta_p$ between optic axis and pump-beam direction. The theoretical dashed curve is discussed in the text.

After the pump beam passed through the ADP crystal its intensity was strongly attenuated by cutoff filters and polaroids. The emitted signal and idler radiation were allowed to pass through an aperture of approximately 2-cm diam located almost 2 m from the ADP crystal and were then focused onto the entrance slit of a monochromator. At different times a visible grating of 64 Å/mm dispersion or an infrared grating of 128 Å/mm dispersion was employed in a monochromator having $f/3.5$ optics. The signal emerging from the monochromator was detected by a photomultiplier. For most of the work an S-1 type photomultiplier was

used because of its fairly uniform response over the wide spectral range in which we were interested. For special purposes, particularly measurements of spectral bandwidths, the greater sensitivity of the S-13 photocathode was required. In all cases, the output voltage from the photomultiplier was displayed on an oscilloscope. The monochromator-photomultiplier detection system was calibrated as a unit, for all combinations of gratings and photomultipliers used, with a standard tungsten lamp (Electro-Optics, Inc., Model L101). With a pivot at the crystal position, the entire detection system could be rotated around the forward pump-beam direction indicated in Fig. 2.

Provision was made to change the properties of the pump beam before it entered the crystal. Apertures of $\frac{1}{4}$, $\frac{3}{16}$, and $\frac{1}{8}$ in. were used to define the area of the beam. A telescope composed of a combination of a convex and

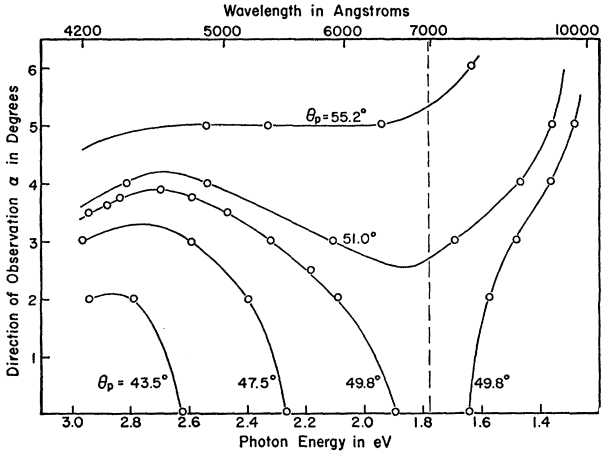


FIG. 4. Photon energy of the scattered radiation is plotted for fixed crystal settings as a function of observation direction $\alpha$. The external angles $\theta_p$ are given as parameters.

a concave lens increased the intensity $P/A$ (power/area) of the beam while leaving it collimated. The total power was changed by known amounts through the use of calibrated attenuators consisting of solutions of $NiSO_4$ and Corning glass filters.

The pump power at high levels was determined by measuring the energy of a pulse with a ballistic thermopile (TRG, Model 100) and a nanovoltmeter (Keithley Instruments, Inc., Model 148) and dividing by a pulse duration of 20 nsec. Since the laser output does exhibit some small fluctuations and because second-harmonic generation amplifies any such variations, the power of the 3472-Å pump beam was monitored by reflecting a small amount of the light into an RCA 922 phototube. With both the monitor and the parametric output displayed on a dual-beam oscilloscope, it was possible to normalize all values to constant input. In fact, however, the corrections rarely exceeded 5%, and the monitor served mainly as an assurance that there were no sudden or gradual changes in the input power.

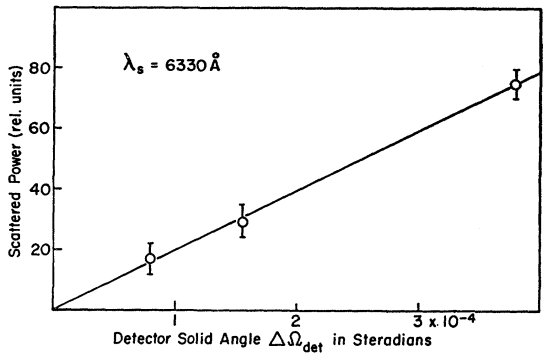


FIG. 5. Scattered power of a fixed signal frequency in the forward direction is measured as a function of the detector solid angle $\Delta\Omega_{det}$.

## EXPERIMENTAL RESULTS

The experimental tuning curves are shown in Fig. 3. For a given observation direction $\alpha$ with respect to the pump-beam direction [see Figs. 1(a) and 1(b)], signal or idler radiation was identified by fixing the monochromator setting and observing the increase of the photomultiplier output above the background as the crystal was rotated through the phase-matching direction $\theta_p$ over a series of laser shots. By repeating this procedure for a variety of wavelengths and observation directions, the tuning curves of Fig. 3 were obtained. The relative crystal orientation in degrees is plotted against the signal or idler photon energy. The approximate actual value of $\theta_p$ is shown at the right. The parameter of the curves drawn is the observation direction $\alpha$ in degrees. All angles are measured outside the crystal. A perpendicular to the crystal faces makes an angle of 52.6° with the optic axis. The dashed curve will be explained in the next section. The polarization of the signal and idler waves was verified to be that of ordinary rays with the pump traversing the crystal as an extraordinary ray.

As demonstrated in Fig. 3 parametric scattering in ADP spans an enormous range of visible and near-infrared wavelengths and a rather large range of

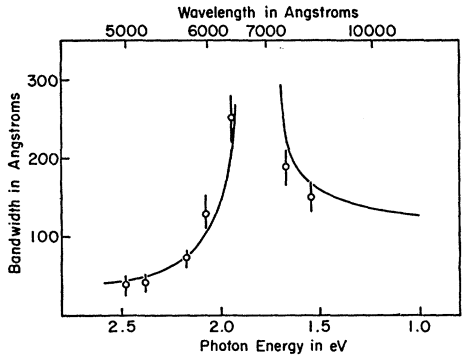


FIG. 6. Bandwidth (full width at half-height) of the scattered radiation is plotted versus the photon energy of the scattered light. The solid line is a best fit of the data points by Eq. (3).

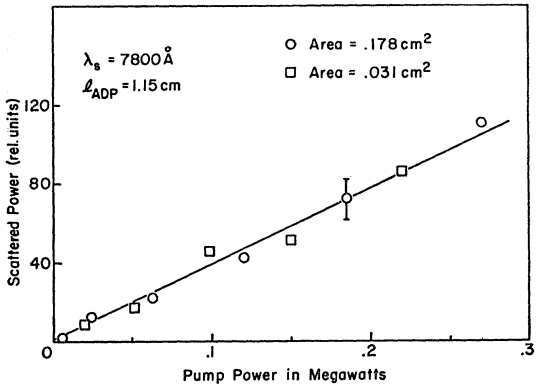


FIG. 7. Scattered power is plotted versus the incident pump power for a fixed photon energy and crystal length. Data points correspond to two beams of different cross sectional area of the incident pump light.

observation angles. A limit to the detection of idler radiation below 1.2 eV (10 000 Å) was set by the loss of sensitivity in the photomultiplier. At photon energies above 2.75 eV (4500 Å) striking anomalous behavior of the tuning characteristics sets in. In this region the signals gradually diminished in power until they could no longer be resolved from the background of scattered light.

For a given crystal orientation, say $\theta_p \approx 49°$, examination of a horizontal slice through Fig. 3 reveals the following information. For the signal side of Fig. 3, i.e., above 1.78 eV, a cone of reddish light is emitted along the forward direction and is surrounded by rings of yellow (near $\alpha = 2°$) and green (near $\alpha = 3°$) light. Then an abrupt cutoff occurs at about $\alpha = 3\frac{1}{2}°$. On the other hand, for a crystal setting at $\theta_p \approx 51°$ no light is emitted in the forward direction. A dark central cone extends out to $\alpha = 2\frac{1}{2}°$ and then concentric red, yellow, and green bands are seen, again with a sharp cutoff around 4° in the blue-green. Overlapping this structure are cones and bands of red and infrared idler radiation, also seen in Fig. 3.

This information is presented quantitatively in Fig. 4. Here the observation angle $\alpha$ (in degrees) at which each signal and idler frequency is observed is plotted against the photon energy for a variety of fixed crystal

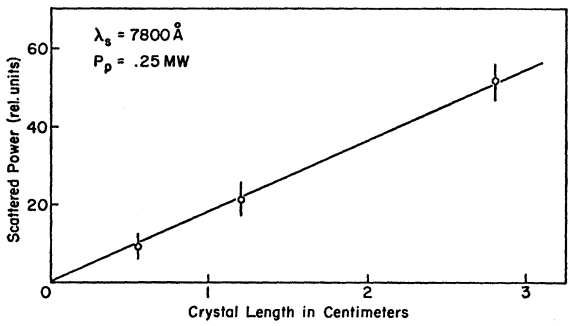


FIG. 8. Scattered power is plotted versus the length of ADP crystals for fixed photon energy and incident pump power.

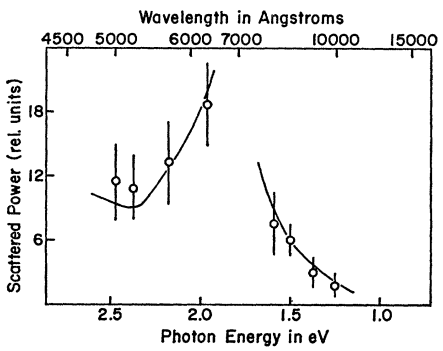


FIG. 9. Scattered power is plotted for a fixed set of conditions versus the photon energy of the scattered light. The solid line is proportional to $\omega^2 \mid \partial\omega/\partial\theta_p \mid_{\theta p}$.

orientations $\theta_p$. Note that there exists a maximum angle at which signal (but not idler) radiation is emitted. This angle is not, however, the limit to higher photon energies of the attainable signal radiation. As a consequence two different signal-photon energies are scattered into the same observation direction in certain cases. This behavior is just another manifestation of the anomalous behavior of the tuning curves beyond 2.75-eV (4500 Å) photon energy in Fig. 3.

A variety of other measurements was undertaken in the forward (pump-beam) direction with the detector intercepting a solid angle $\Delta\Omega_{\text{det}}$ of radiation centered about the pump-beam direction.

Figure 5 shows the experimental dependence of the scattered power upon the solid angle of the detector $\Delta\Omega_{\text{det}}$ at fixed scattered-photon energy and fixed pump-input power.

For the remaining measurements the detector solid angle was fixed at $\Delta\Omega_{\text{det}} \approx 8 \times 10^{-5}$ sr, which corresponds to a linear half-apex angle $\Delta\alpha_{\text{det}}$ of about 5 mrad.

The bandwidth (full width at half-height) of signal

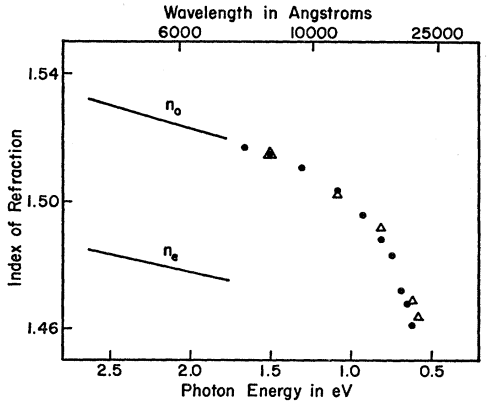


FIG. 10. Index of refraction of ADP is plotted versus photon energy. The points are index values of the idler radiation obtained from the data of Fig. 3 through the use of energy and momentum conservation and the known value of the index at pump- and signal-photon energies. The circles are calculated from data obtained at $\alpha = 0°$; triangles from $\alpha = 4°$. Absorption measurements indicate an absorption constant of 16 $cm^{-1}$ at 0.69 eV (1.8 $\mu$) and 60 $cm^{-1}$ near 0.5 eV (2.5 $\mu$).

and idler radiation was measured. The results are shown in Fig. 6. The calculated curve will be discussed below.

At a fixed idler wavelength of 7800 Å the dependence of the scattered power on the pump-beam power and intensity, and on the length of the ADP crystal, was investigated. Figures 7 and 8 show the experimental results. The output as shown in Fig. 7 was found to be linearly dependent on the pump power and independent of the cross-sectional area or intensity ($I=P/A$) of the beam. Figure 8 shows that, for the crystal lengths investigated, the scattered power is linearly dependent on crystal length. In both cases the scattered power referred to is the total power received over the whole solid angle of the detector and the entire spectral bandwidth.

The dependence of the scattered power of signal and idler on the frequency position within the tuning range was measured and is shown in Fig. 9. Again it is the integrated total power which was recorded. The theoretical curve will be discussed later.

Finally, an absolute measurement of the parametric scattered power was undertaken. At 7800 Å, scattered power of 1 $\mu$W was recorded for a 1.15-cm crystal and a pump power of 0.25 MW.

## INTERPRETATION OF EXPERIMENTAL RESULTS

For a comparison of the experimental results with theory, the results of a scattering theory of optical parametric scattering by Giallorenzi and Tang[3] will be summarized here. The power scattered by a nonlinear crystal at photon energy $\hbar\omega_s$ into a solid angle $\Delta\Omega_{\rm det}$ of the detector is given by

$$P_s=\frac{(\Delta\epsilon_1)^2\hbar\omega_s^2\omega_i}{2\pi c^4 n_s^o n_i^o \omega_p \left|\partial n_p^e(\theta)/\partial\theta_p\right|_{\theta_p}} \times(\omega_s^2)\,(\Delta\omega_s^\theta/\Delta\theta_{\rm inc})\,(P_p L\Delta\Omega_{\rm det}), \quad (1)$$

where $L$ is the crystal length, $P_p$ is the total pump power, $\Delta\omega_s^\theta$ is that part of the frequency bandwidth which is due to the divergence of the pump beam (the total bandwidth seen by a finite detector $\Delta\omega_{\rm det}$ is larger than $\Delta\omega_s^\theta$), $\theta_p$ is the angle between the optic axis and the mean pump direction, and $\Delta\theta_{\rm inc}$ is the incident pump-beam divergence outside the crystal. The $n_s^o$ and $n_i^o$ are the indices of refraction for the ordinary ray for signal and idler, respectively, and $n_p^e$ is the index of refraction of the extraordinary ray. For measurements taken along the forward direction (pump-beam direction), $\Delta\omega_s^\theta/\Delta\theta_{\rm inc}$ is simply given by the average slope of the tuning curve of Fig. 3 for $\alpha=0$, i.e., $\partial\omega_s/\partial\theta_p$. The coefficient $\Delta\epsilon_1$ is related to the nonlinear susceptibility and is given by

$$\Delta\epsilon_1=4\pi\chi_{xyz}\sin\theta_p.$$

The tuning characteristics of the parametric process are determined by the equation

$$F=\omega_p-\omega_s-[1/n_o(\mathbf{k}_p-\mathbf{k}_s)][n_e^2(\mathbf{k}_p)\omega_p^2+n_o^2(\mathbf{k}_s)\omega_s^2 -2n_o(\mathbf{k}_s)n_e(\mathbf{k}_p)\omega_p\omega_s\hat{k}_s\cdot\hat{k}_p]^{1/2}=0, \quad (2)$$

where $n_o$ is the index of refraction for the ordinary wave, and $\mathbf{k}_s$ and $\mathbf{k}_p$ are the wave vectors for the signal and pump light, respectively.

*The tuning curves.* Consider the solutions of Eq. (2) for a given observation direction, i.e., for specified directions of $\hat{k}_s$ and $\hat{k}_p$. In this case Eq. (2) relates $\omega_s$ to $n_e(\mathbf{k}_p)$. In turn, $n_e(\mathbf{k}_p)$ can be changed by rotating the crystal, i.e., by changing $\theta_p$. Equation (2) therefore predicts a tuning curve, that is, pairs of values of $\omega_s$ and crystal orientation $\theta_p$. For the collinear case ($\hat{k}_p\cdot\hat{k}_s=1$ or $\alpha=0$) it is known[9] that the solution of Eq. (2) is a parabolic dependence of $\theta_p$ on $\omega_s$ near the degenerate frequency $\omega_s=\omega_i=\frac{1}{2}\omega_p$. The dashed curve of Fig. 3, fitted to the data points, is parabolic and its position is consistent with the known dispersion curve for ADP.

It is also possible to fix the crystal orientation $\theta_p$, thus determining $n_e(\mathbf{k}_p)$. Equation 2 then gives a relation between $\omega_s$ and the direction of observation $\hat{k}_s$ and therefore predicts the angular dependence of the emitted radiation as shown in Fig. 4. Again it has been shown[10] analytically that for small angles $\alpha$ the dependence should be quadratic. Figure 4 is consistent with this prediction.

From Eq. (2) the exact tuning curves can be calculated if the indices of refraction of the nonlinear crystal are sufficiently well known. We have not done that. (We would like to point out, however, that the gross features of predictions made by Giallorenzi and Tang[3] on the basis of such calculations are all borne out by the experiments.) Rather we have used the data of the tuning curves to calculate indices of refraction for ADP in regions where measurements were not available.

We took the known values of the indices of ADP for the signal- and pump-photon energies and calculated, with the use of Eq. (2) and the tuning curves of Fig. 3, the ordinary index of the corresponding idler radiation. The values obtained from two of the tuning curves, $\alpha=0°$ and $\alpha=4°$, are shown in Fig. 10. There is rather good agreement between these independent sets of calculated values. The solid lines are the known[11] dispersion curves of ADP for ordinary and extraordinary rays. It should be noted that the absorption constant for the sample of ADP used in the experiment reaches the inverse of the crystal length (1 cm) at about 1.0 eV (1.25 $\mu$). At 0.69 eV (1.8 $\mu$) the absorption constant is about 16 cm$^{-1}$ and beyond that it reaches a plateau of around 60 cm$^{-1}$ in the region near 0.5 eV (2.5 $\mu$). It can be seen from Fig. 10 that the anomalies in the tuning curves above 2.75-eV photon energy are caused by the onset of anomalous dispersion in the infrared below 0.80 eV. Parametric scattering, then, provides a direct way of measuring the real part

[9] A. Yariv and W. H. Louisell, IEEE J. Quantum Electron. **QE-2**, 418 (1966).

[10] R. G. Smith, J. G. Skinner, J. E. Geusic, and W. G. Nilsen, Appl. Phys. Letters **12**, 97 (1968).

[11] Data by T. Teska were made available to us by the Clevite Corporation.

of the index of refraction in the absorptive region of a crystal through use of the phase-matching conditions.

*Bandwidth.* For a given direction of signal radiation $\mathbf{k}_s$, Eq. (2) predicts a different signal frequency $\omega_s$ for each $\mathbf{k}_p$. Since the pump-beam divergence necessarily results in a range of $\mathbf{k}_p$, there will be a bandwidth $\Delta\omega_s^{\theta}(\mathbf{k}_s)$ different in each direction of observation $\mathbf{k}_s$, due solely to the divergence of the pump beam. This is the quantity which appears in Eq. (1). On the other hand, even if one had a perfectly collimated pump beam, any detector of finite aperture would detect a range of signal frequencies $\Delta\omega_s^{\alpha}$ because $\omega_s$ depends on $\alpha$. In practice, the detected frequency bandwidth $\Delta\omega_{\text{det}}$ is a function of both effects, and in typical experiments the two contributions are often of comparable importance. The two effects are not independent and the exact solution is not cylindrically symmetric about the mean pump direction.[3] It is possible, in principle, to treat the problem exactly by looking for solutions of Eq. (2) over the range of $\alpha$ and $\theta_p$. Since our experiments are not able to resolve such fine details, we have attempted to fit the data with an approximate curve of the form

$$\Delta\omega_{\text{det}}=\Delta\omega_s^{\theta}+\Delta\omega_s^{\alpha}$$
$$=(\partial\omega_s/\partial\theta_p)_{\theta_p}\Delta\theta_{\text{inc}}+(\partial\omega_s/\partial\alpha)_{\alpha}\Delta\alpha. \quad (3)$$

It should be noted that $(\partial\omega_s/\partial\alpha)_{\alpha}$ is different for signal and idler frequencies. (See the curves for $\theta_p=49.8°$, for example, in Fig. 4.) In Eq. (3), $\Delta\alpha$ is experimentally controllable, while the required partial derivatives may be obtained from the experimental tuning curves shown in Figs. 3 and 4. The only unknown quantity is, then, $\Delta\theta_{\text{inc}}$, which enters into the output power formula (1). In our experiment $\Delta\alpha$ is the half-apex angle of the detector solid angle and is 5 mrad. The solid curve of Fig. 5 was fitted to the data points by choosing $\Delta\theta_{\text{inc}}=2.5$ mrad, a value typical of a rather "good" ruby laser.

*Scattered power.* Equation (1) predicts that the detected output power should vary linearly with the detector solid angle (for detectors which are not too large), with the total pump power (below the threshold for stimulated processes), and with the crystal length. These predictions are borne out by the data presented in Figs. 5, 7, and 8, respectively. Figure 5 shows the expected dependence upon the detector solid angle. Figure 7 shows that the output is proportional to the total pump power and independent of the pump area and intensity ($I=P_p/A$). Figure 8 shows a linear dependence on length.

The dependence of the detected signal or idler power on the frequency of the observed radiation is somewhat more complicated. The factor

$$\frac{(\Delta\epsilon_1)^2\hbar\omega_s^2\omega_i}{2\pi c^4 n_s^o n_i^o \omega_p\,|\,\partial n_p^e(\theta)/\partial\theta_p\,|_{\theta_p}},$$

however, turns out to be almost constant over a wide spectral range ($\pm 9\%$ in the range 4500–15 000 Å). The frequency dependence of the output is therefore dominated in the region of our experiments by the factor $\omega_s^2\Delta\omega_s^{\theta}/\Delta\theta_{\text{inc}}$. Away from the degenerate frequency, for small $\Delta\theta_{\text{inc}}$, we may approximate $\Delta\omega_s^{\theta}/\Delta\theta_{\text{inc}}$ by the inverse slope of the tuning curve. Multiplying, then, the experimental values of $(\partial\omega_s/\partial\theta_p)_{\theta_p}$ in Fig. 3 by $\omega_s^2$, we are able to fit the experimental results by the predicted frequency dependence of Eq. (1), as shown by the solid curve in Fig. 9.

The data and the theoretical curve presented in Fig. 9 do not extend into the "anomalous" region beyond 2.75 eV (4500 Å). Experimentally, it was observed that at these short wavelengths the intensity diminished until it was no longer discernible above the background. This decrease in intensity can be largely accounted for by a decrease in $\Delta\omega_s^{\theta}$, since $(\partial\omega_s/\partial\theta_p)_{\theta_p}$ is small for a steep tuning curve such as is observed in Fig. 3 near 2.9 eV (4300 Å). In addition, however, for these signal frequencies the complementary idler radiation is strongly absorbed and it becomes necessary to consider possible dispersion of the nonlinear susceptibility and even to reexamine the entire derivation of (1). At the present time experimental accuracy does not allow us to separate these two effects.

*Absolute power output.* From Eq. (1) the scattered output power was calculated. The following values of quantities were determined in this experiment: $\omega_s=2.4\times10^{15}$ sec$^{-1}$, $\omega_i=3.0\times10^{15}$ sec$^{-1}$, $\omega_p=5.4\times10^{15}$ sec$^{-1}$, $P_p=2.5\times10^5$ W, $\Delta\theta_{\text{inc}}=2.5$ mrad, $\Delta\omega_s^{\theta}=5.0\times10^{13}$ sec$^{-1}$, $\Delta\Omega_{\text{det}}=8\times10^{-5}$ sr. The values of $n\approx1.5$ and $\Delta\epsilon_1=1.3\times10^{-8}$ esu ($5.8\times10^{-12}$ mV$^{-1}$ mks) were obtained from the literature. The calculated scattered output was 2 $\mu$W compared to a measured value of 1 $\mu$W.

## CONCLUSION

Complete agreement was found between theory and experiment of the dependence of the parametric scattering process, including the frequency, bandwidth, and intensity of the scattered radiation, on crystal orientation, observation direction, pump power, crystal length, and detector aperture. The quantitative measurement of the total scattered power was in reasonable agreement with theoretical predictions.

The parametric process of ADP pumped at 3472 Å covers a wide range of visible and infrared wavelengths and can be observed over a rather large range of observation directions. For a peak power of 1 MW about 1–10 $\mu$W of scattered radiation can be obtained in 1-cm-long crystals with a detector aperture of about $10^{-4}$ sr.

## ACKNOWLEDGMENTS

The authors would like to thank T. G. Giallorenzi and Professor C. L. Tang for making available a copy of their work and for several helpful discussions. The help of R. Scarlet with some of the measurements is thankfully acknowledged.